Scattering Center Determination for Integrated Antenna Measurements at mm-Wave Frequencies

Linus Boehm and Christian Waldschmidt
Institute of Microwave Engineering
Ulm University
Ulm, Germany
linus.boehm@uni-ulm.de

***Abstract*—In this paper the results of integrated antenna measurements are analyzed to identify the main reflection locations when measuring with wafer probes. Two different approaches are described and the measurement results for two different probe designs are shown. First, the main reflection center on the wafer probe is determined by analyzing the measured far field radiation pattern at 160 GHz. The second approach is based on an extrapolation measurement of the antenna. It is shown that the reflective areas can be identified for both probe designs. The results can be used to assess the measurement uncertainty and to quantify the measurement error.**

I. Introduction

On-chip antennas are becoming more and more important for integrated radar sensors and communication MMICs to avoid lossy off-chip transitions. However, both feeding the antenna under test (AUT) and measuring the radiated fields is challenging, due to the small wavelength and antenna dimensions of less than 1 mm. Wafer probes have to be used to contact and feed integrated antennas [1]. These probes are primarily made from metal and thus present a comparably big reflective surface in the immediate vicinity of the AUT [2]. The reflections from the wafer probe cause ripples in the radiation pattern and large deviations in gain measurements that depend on the measurement distance and the relative positions of reflector and antenna. [3] performs near field scans to avoid reflections from surrounding objects, however, the wafer probes limit the scanning range during near field measurements [4], reducing the overall measurement accuracy.

In [2] the probe is moved underneath the measurement surface in order to reduce reflections and distortions by bending the printed circuit board (PCB). While reducing reflections significantly at 60 GHz, this approach is not applicable for on-chip antennas as the substrate is way smaller than a PCB and cannot be bent. A different approach was taken in [5], where the wafer probe was modified such that the probe body is underneath the antenna plane by extending and bending the coaxial probe tip. With this probe the disturbing effects were reduced at approximately 60 GHz, but custom probe designs are pricey and bended probe tips are difficult to fabricate at high frequencies.

For a better understanding of the probe influence on the measurement results, the main points of reflection are identified in this paper with two different methods. The results can be used for future probe designs that are better suited for integrated antenna measurements.

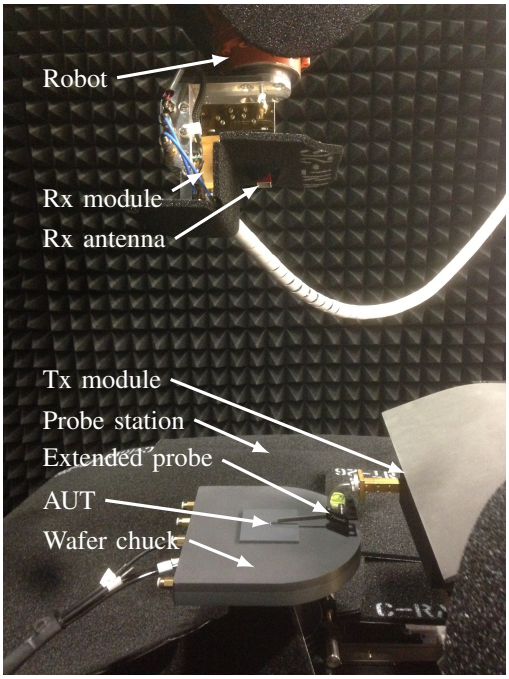

Fig. 1. Measurement setup with robot, converter module, and probe station.

The setup is briefly described in Section II. In Section III-A, the scattering center is determined by analyzing the measured radiation pattern and in Section III-B an extrapolation measurement is used. All measurements were done at 160 GHz with two different wafer probe designs.

II. Measurement Setup

The measurement setup is shown in Fig. 1 and detailed description can be found in [6]. It uses an industrial robotic arm to precisely move the reference antenna around the AUT and probe the radiated field at the desired measurement points. With the robotic arm it is possible to perform near field, far field, and polarization measurements as well as extrapolation measurements, where the field is measured over the separation distance between reference antenna and AUT. The robot triggers a vector network analyzer (VNA) whenever a

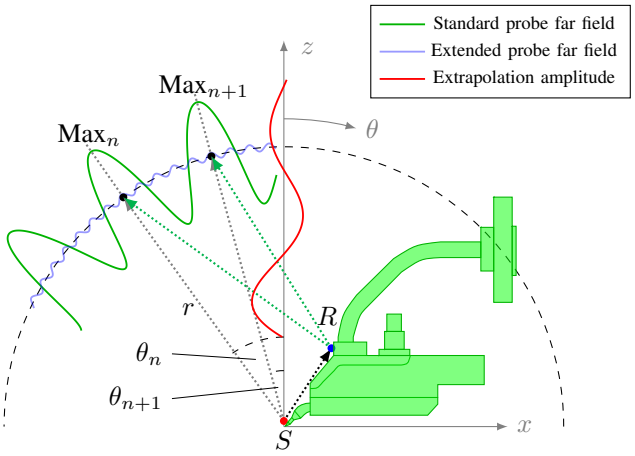

Fig. 2. The effect of probe reflections in far field and extrapolation measurements.

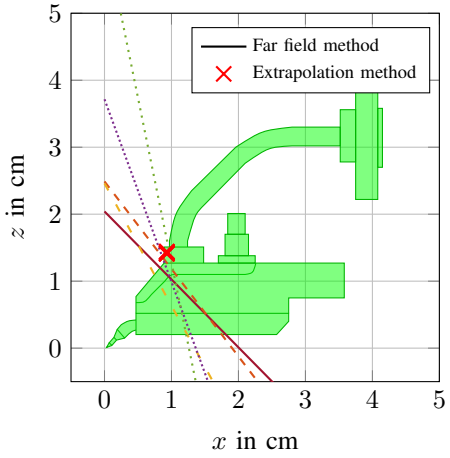

Fig. 3. Determined scattering center locations for the standard probe at 160 GHz with both methods.

specified measurement position is reached. Converter modules are required to extend the frequency range of the VNA and wafer probes are used to contact the chip and feed the signals to the AUT.

Two different wafer probe models were compared. The first one is a standard off-the-shelf wafer probe, while the second one is custom made, designed for improved antenna measurements. Due to the small chip dimensions, the wafer probes are located right next to the radiating element, what causes severe distortions during measurements. In order to decrease reflections and shading, the dedicated antenna measurement probe (see Fig. 1) has an extended coaxial feed to increase the distance between AUT and the reflective probe surface and thus reduce distortions.

III. Scattering Center Determination

Two different methods to determine the scattering center were used. The first method is based on a far field measurement [7], while the second method uses an extrapolation measurement.

A. Far Field Pattern Analysis

The biggest effects of probe reflections can be seen when measuring in probe direction, i.e. the x-z-plane in Fig. 2. The reflections interfere with the desired field components on the measurement plane and this interference causes constructive and destructive interference depending on the relative phase between direct and reflected signal.

A maximum occurs when the path difference between direct and reflected signal is $\Delta_{\text{path}} = (2n-1)\cdot\lambda/2$, as the phase of the reflected signal changes by π when being reflected.

As the measurement is taken on a sphere around the AUT, the path length of the direct signal is constant during the measurement. Assuming that the location of the reflection does not change over θ, the only path length that depends on θ is the path from the scattering center R to the measurement surface. Therefore, the distance between scattering center and measurement location has to change by λ between two adjacent maxima:

$$\Delta_{\text{path}} = \left| l_{R\to\max_n} - l_{R\to\max_{n+1}} \right| \stackrel{!}{=} \lambda\,. \tag{1}$$

The distance between the point of reflection and the measurement surface can be calculated with

$$l_{R\to\max_m} = \sqrt{(R_x + r\sin\theta_m)^2 + (r\cos\theta_m - R_z)^2}, \tag{2}$$

where R_x and R_z is the x and z location of the scattering center and r is the measurement radius.

By solving (1) with (2) for R_z, the z position for different R_x values can be calculated for a given pair of adjacent maxima. This yields a line of possible reflection centers for each maxima pair. The intersection point of these lines is the scattering center.

Figure 3 shows the calculated lines for an integrated antenna measurement at 160 GHz. The lines intersect with one another and with the probe surface at the transition between probe body and waveguide connector, clearly illustrating the main source of reflection when measuring with the standard wafer probe.

When measuring with the extended probe, the distance between reflective surface and AUT is increased, which is why the path length changes faster over θ, thus increasing the number of maxima on the measurement surface as indicated in Fig. 2. With a higher number of maxima, more lines of possible scattering centers can be calculated. The results are shown in Fig. 4. Compared to the standard probe, the intersection points of the reflection lines show a higher variation, which is due to the smaller peak-to-peak amplitude of the ripples when measuring with the dedicated probe. While the large ripples of the standard probe allow to determine the position of the maxima with high accuracy, the small ripples caused by reflections from the extended probe are more difficult to detect as reflections from other objects that superimpose with the probe reflections have a bigger impact on the measurement

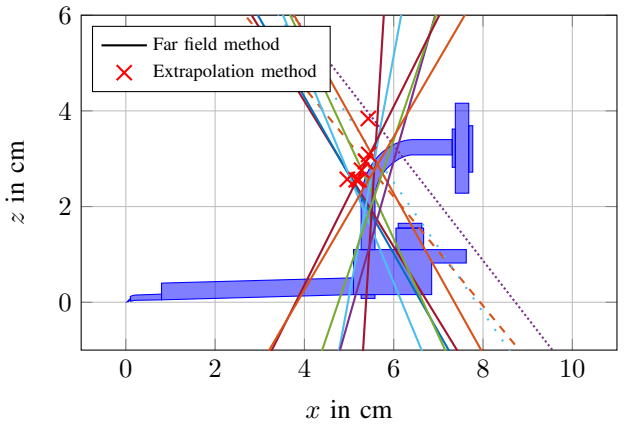

Fig. 4. Determined scattering center locations for the extended probe at 160 GHz with both methods.

results. However, it is still possible to identify the main point of reflection at the bend of the waveguide connector of the probe.

B. Extrapolation Measurement

During an extrapolation measurement, the received signal is measured in boresight direction as a function of the separation distance between AUT and reference antenna. To prevent collisions of the Rx antenna with the wafer probe an open waveguide near field probe was used as Rx antenna. The smaller aperture of the near field probe compared to a standard gain horn allows to decrease the minimum measurement distance to 1.5 cm without colliding with the wafer probe. For this analysis the distance was changed from 1.5 cm to 80 cm. Due to the reflections and the resulting interference, the measured signal has ripples that depend on the location of the reflection center. The amplitude of the superimposed signal A_{total} can be calculated with

$$\begin{aligned} A_{\text{total}} &= A_{\text{direct}} + A_{\text{reflected}} \\ &= \frac{\lambda}{4\pi l_{\text{direct}}} + \frac{\lambda G_{\text{refl}}}{4\pi l_{\text{refl}}} \cdot \mathrm{e}^{\mathrm{j}k(l_{\text{direct}} - l_{\text{refl}})}, \end{aligned} \tag{3}$$

where k is the wavenumber, G_{refl} is the gain of the reflected signal, and l_{direct} and l_{refl} are the path lengths of the direct and the reflected signal, respectively. G_{refl} takes into account the amplitude change caused by the reflection itself as well as the higher free space attenuation due to the longer path of the reflected signal compared to the direct path.

The point of reflection can be estimated by choosing the x and y location of the scattering center such that the difference between A_{total} and the measured S_{21} is minimized. In this case the optimization variables were the position x and y, G_{refl}, and a normalization factor.

Figure 5 shows the results of the extrapolation measurement and the calculated magnitude of the superimposed signal for the standard wafer probe. Due to the close proximity of the reflection center to the AUT, the biggest ripples can be seen within a distance of less than 10 cm. For larger distances the

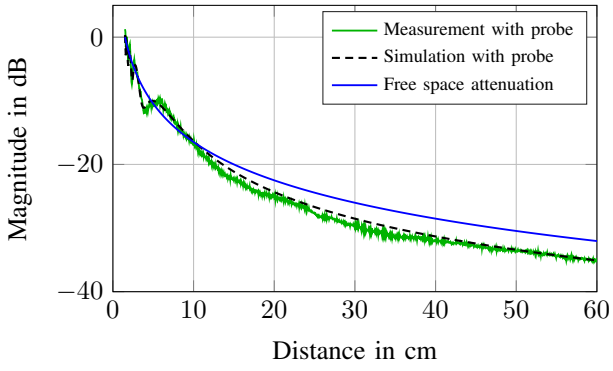

(a) Overview (1.5 cm to 80 cm)

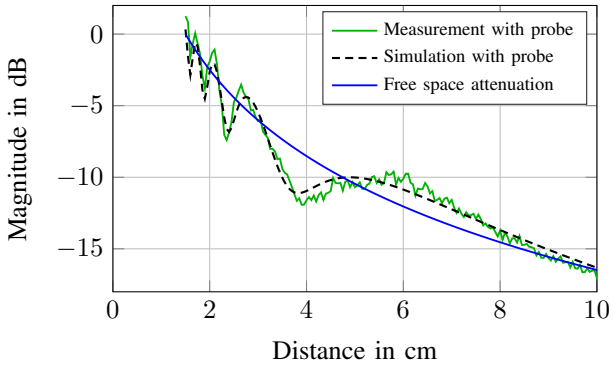

(b) Detailed view (1.5 cm to 10 cm)

Fig. 5. Measured extrapolation magnitude with the standard probe at 160 GHz.

slope of the measured signal is approximately equal to the free space attenuation, which means that most information about the point of reflection can be obtained from the measurement results below 10 cm. As long as these results are taken into account for the calculation, the deviation between the calculated scattering center positions is less than 1 mm. Figure 3 indicates the calculated scattering centers as red crosses for the evaluation ranges shown in Table I.

Figure 6 shows the same measurement when contacting with the extended probe. Up to a distance of 10 cm the ripples of Fig. 5b are not present. Because of the increased distance between scattering center and AUT, the ripples can be seen at higher distances, mainly between 20 cm and 50 cm. In this case the best results can be obtained when disregarding the first 10 cm, where the distortions are not primarily caused by the probe reflections. The calculated scattering centers are indicated in Fig. 4.

The calculated reflection positions as well as the resulting standard deviations are shown in Table I. The highest accuracy can be achieved when only those distances are taken into account, where the characteristic ripples occur. For reflections close to the AUT, smaller distances should be evaluated. When the reflection occurs further away from the AUT, larger distances yield better results.

TABLE I
CALCULATED SCATTERING CENTERS (ALL UNITS IN CM)

								Standard deviation
	Standard probe							
Evaluation range	0…20	0…30	0…40	0…50	0…60	0…70	0…80	
Calculated position (x,z)	(0.93, 1.41)	(0.93, 1.41)	(0.93, 1.41)	(0.93, 1.42)	(0.93, 1.43)	(0.93, 1.44)	(0.93, 1.44)	($<$0.1, $<$0.1)
	Extended probe							
Evaluation range	10…80	20…80	30…80	40…80	50…80	60…80	70…80	
Calculated position (x,z)	(5.28, 2.76)	(5.37, 2.94)	(5.44, 3.09)	(5.16, 2.56)	(5.43, 3.84)	(5.22, 2.56)	(4.96, 2.57)	(0.2, 0.5)

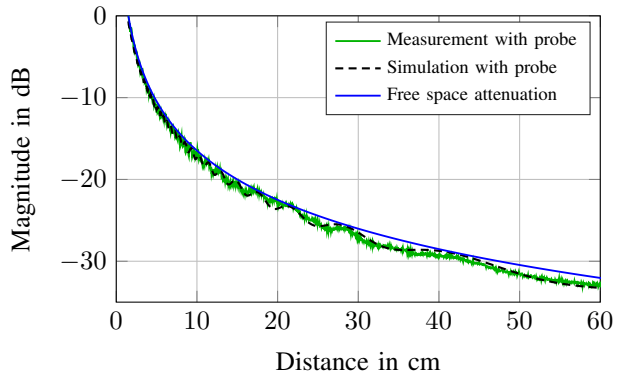

(a) Overview (1.5 cm to 80 cm)

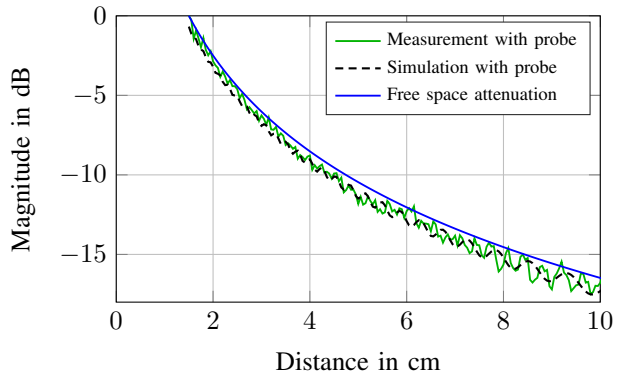

(b) Detailed view (1.5 cm to 10 cm)

Fig. 6. Measured extrapolation magnitude with the extended probe at 160 GHz.

IV. Impact on Gain Measurements

As shown in Figs. 5 and 6, the reflections cause deviations from the expected free-space path loss of the measured signal. This leads to erroneous results during gain measurements. The error depends on the location of the reflector, the measurement frequency, and the measurement distance. These reflections are the biggest source of uncertainty in gain measurements with a standard deviation of 0.83 dB as it was shown in [8].

The effect can be reduced significantly when measuring with the dedicated antenna measurement probe. In this case the ripples are much smaller and the deviations from the free space path loss are reduced, which indicates smaller reflections.

V. Conclusion

In this paper reflections of wafer probes during integrated antenna measurements were analyzed. Two different methods to determine the main scattering centers of wafer probes were shown and both methods were applied to antenna measurements at 160 GHz with two different wafer probes.

One method is based on the measured radiation pattern and the second one on an extrapolation measurement. It was shown that the main point of reflection can be identified with both methods for different probe designs. The best results can be achieved, when only those distances where the characteristic ripples of the superimposed signal occur are analyzed. If the reflection appears close to the AUT, small distances have to be taken into account for an accurate evaluation. When the point of reflection is further away from the AUT small distances can be neglected.

Acknowledgment

This work was supported by the German Research Foundation (DFG) under the project number WA 3506/1-1.

References

[1] E. C. Lee, E. Szpindor, and W. E. McKinzie III, "Mitigating Effects of Interference in On-Chip Antenna Measurements," *AMTA 37th Annual Meeting and Symposium, Long Beach, California, USA*, 2015.

[2] A. C. F. Reniers, A. R. van Dommele, M. D. Huang, and M. H. A. J. Herben, "Disturbing Effects of Microwave Probe on mm-Wave Antenna Pattern Measurements," in *The 8th European Conference on Antennas and Propagation (EuCAP 2014)*, pp. 161–164, Apr. 2014.

[3] Z.-M. Tsai, Y.-C. Wu, S.-Y. Chen, T. Lee, and H. Wang, "A V-Band On-Wafer Near-Field Antenna Measurement System Using an IC Probe Station," *IEEE Transactions on Antennas and Propagation*, vol. 61, pp. 2058–2067, Apr. 2013.

[4] G. Gentile, V. Jovanovic, M. Pelk, L. Jiang, R. Dekker, P. de Graaf, B. Rejaei, L. de Vreede, L. Nanver, and M. Spirito, "Silicon-filled rectangular waveguides and frequency scanning antennas for mm-wave integrated systems," *IEEE Transactions on Antennas and Propagation*, vol. 61, pp. 5893–5901, Dec. 2013.

[5] A. Reniers, A. van Dommele, A. Smolders, and M. Herben, "The Influence of the Probe Connection on mm-Wave Antenna Measurements," *IEEE Transactions on Antennas and Propagation*, vol. 63, pp. 3819–3825, Sept. 2015.

[6] L. Boehm, S. Pledl, F. Boegelsack, M. Hitzler, and C. Waldschmidt, "Robotically Controlled Directivity and Gain Measurements of Integrated Antennas at 280 GHz," in *European Microwave Conference (EuMC), Paris, France*, Sep. 2015.

[7] L. Boehm, M. Hitzler, F. Roos, and C. Waldschmidt, "Probe Influence on Integrated Antenna Measurements at Frequencies Above 100 GHz," in *European Microwave Conference (EuMC), London, UK*, Oct. 2016.

[8] L. Boehm, F. Boegelsack, M. Hitzler, S. Wiehler, and C. Waldschmidt, "Accuracy Evaluation for Antenna Measurements at mm-Wave Frequencies," in *10th European Conference on Antennas and Propagation (EuCAP)*, pp. 4009–4013, Apr. 2016.